JOURNAL OF CATALYSIS **164,** 315–321 (1996)
ARTICLE NO. 0387

Preparation and CO_2 Methanation Activity of an Ultrafine Ni(II) Ferrite Catalyst

Masamichi Tsuji,*[,1] Tatsuya Kodama,† Takashi Yoshida,* Yoshie Kitayama,† and Yutaka Tamaura*

*Department of Chemistry, Research Center for Carbon Recycling and Utilization, Tokyo Institute of Technology, Ookayama, Meguro-ku, Tokyo 152, Japan; and †Department of Chemistry and Chemical Engineering, Faculty of Engineering, Niigata University, 8050, Ikarashi, 2-nocho, Niigata 950-21, Japan

Received September 18, 1995; revised June 21, 1996; accepted July 1, 1996

Ultrafine Ni(II) ferrite (UNF) with 36% Ni^{2+} substitution for Fe^{2+} in magnetite has been synthesized in order to study its catalytic activity and selectivity toward CO_2 methanation at 300°C. Ni(II) ferrites were prepared by two different methods: (1) coprecipitation of Ni^{2+}, Fe^{2+}, and Fe^{3+} at 60°C followed by heating to 300°C and (2) oxidation of aqueous suspension of Fe^{2+} and Ni^{2+} hydroxides at 65°C (oxidation method). The BET surface area of the initial UNF synthesized by coprecipitation was 73 $m^2\ g^{-1}$, eight times as large as that of the Ni(II) ferrite obtained by the oxidation method (NF; 9 $m^2\ g^{-1}$). It rapidly decreased to 26 $m^2\ g^{-1}$ by sintering in the initial stage of methanation. The yield of CH_4 obtained on the UNF catalyst was 1.5–6.0 times larger than that on the NF catalyst in a 2-h run of the methanation, depending on a flow rate of reactant H_2/CO_2 mixed gas. It was found that the selectivity for CH_4 was much improved in UNF (96%) in comparison with NF. XRD and chemical analysis showed that the UNF and NF were transformed to oxygen-deficient ferrite forms during the methanation. The specific activity (mol $m^{-2}\ s^{-1}$) of UNF for CH_4 formation was rather lower than that of NF, about half the activity of NF, which could be explained assuming that oxygen sublattice points on the catalyst surface formed by H_2 reduction serve as active sites for methanation. On the other hand, the activity for CO formation significantly decreased on UNF, due to the change in the nature of the active site.

INTRODUCTION

Magnetite and M(II)-bearing ferrites with the spinel-type structure belong to the space group F_{d3m} and form a family of oxygen-deficient spinel ferrites which are generally represented by the formula $M_xFe_{3-x}O_{4-\delta}$; the oxygen deficiency δ expresses the reduction degree of ferrite. The oxygen-deficient ferrite (ODF) can be formed by hydrogen reduction of the ferrite at 300°C,

$$M_xFe_{3-x}O_4 + \delta H_2 \rightarrow M_xFe_{3-x}O_{4-\delta} + \delta H_2O.$$

The ODF is highly reactive and decomposes CO_2 to its elements, i.e., carbon and oxygen, around 300°C (1–10). The former is deposited on the surface of the ferrites and the latter is incorporated into the lattice points of the ODF crystal:

$$M_xFe_{3-x}O_{4-\delta} + (\delta - \delta')/2CO_2 \rightarrow M_xFe_{3-x}O_{4-\delta'} + (\delta - \delta')/2C\ (\delta > \delta').$$

The carbon deposited by CO_2 decomposition can readily react with hydrogen to form CH_4 over the ODF at 200–300°C (2, 11–15):

$$C + 2H_2 \rightarrow CH_4.$$

Thus, CO_2 can be converted to CH_4 through the three reaction steps using ODF. A great number of bivalent metal ferrites ($M_xFe_{3-x}O_4$; M = Fe, Ni, Co, Cu, Zn, Mg, Mn) have been studied for their effect of substitution on their activity for CO_2 methanation. It was found that the substitution of Ni(II) for Fe(II) in magnetite ($Ni_xFe_{3-x}O_4$) strongly improves its activity for CO_2 methanation (11, 14). A high yield, over 86% for CH_4, could be attained through the three steps of the reactions at 200–300°C using Ni(II) ferrite.

When the mixed gas of CO_2 and H_2 is flowed through ferrite, these reactions take place on the ferrite surface and the catalytic conversion of CO_2 to CH_4 can occur over the ODF at 300°C (16–18). However, the yield and selectivity for CH_4 formation were less than 25 and 83%, respectively, at 300°C in the catalytic conversion. One of the most effective ways to improve the methanation efficiency is to use ferrite catalysts with a large surface area, which makes both the H_2 reduction of the ferrite and the methanation of CO_2 via carbon more efficient. The enlargement of the surface area will be accomplished by development of a new method of preparation for ultrafine ferrite particles. The crystallite size of the ferrites can be controlled within the range from 50 to 500 nm by changing the aging time in the conventional oxidation methods reported hitherto (19–28). However, it is difficult to obtain ultrafine ferrites with diameters less than 50 nm by the oxidation method.

[1] To whom correspondence should be addressed. Fax: +81-3-5734-3337. E-mail: mtsuji@chem.titech.ac.jp.

0021-9517/96 $18.00

The objective of the present study is to investigate the catalytic activity and selectivity for methanation of CO_2 of ultrafine Ni(II) ferrite synthesized by coprecipitation.

METHODS

1. Synthesis of Ni(II) Ferrite Catalysts

Ni(II) ferrite catalysts were prepared by two different methods as follows: Ultrafine Ni(II) ferrite (UNF) with 39% Ni^{2+} substitution ($Ni(II)/Fe_{total}$ mole ratio $= 0.15$) was synthesized by coprecipitation, followed by heating of the coprecipitate to 300°C. Appropriate portions of $NiCl_2 \cdot 6H_2O$ (2.09 g), $FeCl_2 \cdot 4H_2O$ (2.68 g), and $FeCl_3 \cdot 6H_2O$ (12.2 g) were dissolved at 60°C in distilled water (0.15 dm^3) previously degassed by passing nitrogen gas through it for a few hours. An appropriate amount of NaOH (7.20 g) was separately dissolved in degassed water and the NaOH solution was kept at 60°C. The mixed metal chloride solution was added to the NaOH solution at 60°C with vigorous stirring for coprecipitation. The formed coprecipitate was aged for 1 h at 60°C by bubbling nitrogen gas in the mother solution.

Ni(II) ferrite with a crystallite size of 100–200 nm (NF) was prepared by oxidation of aqueous suspension of Fe(II) and Ni(II) hydroxides according to our papers reported previously (21–28). Requisite quantities of $NiSO_4 \cdot 6H_2O$ (44.1 g) and $FeSO_4 \cdot 7H_2O$ (312 g) were dissolved in water previously degassed by passing nitrogen gas through distilled water (4.0 dm^3) for a few hours: the $Ni(II)/Fe_{total}$ mole ratio was 0.15. The pH of the solution was raised to 9.0 by adding an NaOH solution to form hydroxide suspension. Air was passed through the hydroxide suspension to oxidize them at 65°C. The pH was kept constant at 9.0 by adding the 3.0 mol dm^{-3} NaOH solution. The end of the oxidation was recognized by means of an oxidation-reduction potential (ORP) measurement (22).

The products thus synthesized by the coprecipitation and oxidation methods were collected by centrifuging at 14,000 rpm. After washing with distilled water and successively with acetone, they were dried *in vacuo* at 60°C for a day. The products were then heated in an N_2 gas stream at 300°C for 1–2 h to remove H_2O and any OH^- groups incorporated.

2. Characterization of the Catalysts

The products were identified by X-ray diffractometry (XRD) with Cu$K\alpha$ radiation (Rigaku, Model RINT 2000). The infrared (IR) spectra of the products were recorded by the KBr disc technique (Shimadzu, Model FTIR-8500). The Mössbauer spectra were recorded at room temperature with a ^{57}Co source diffused in metallic rhodium which was oscillated in a constant acceleration mode. The Doppler velocity scale was calibrated with thin absorbers of α-Fe foil. The spectra were analyzed by a computer curve fitting method assuming pure Lorentzian line shapes. The chemical compositions were determined both by inductively coupled plasma (ICP) spectroscopy (Seiko Instruments, Model SPS7000) and by colorimetry (HITACHI, Model U-1100) using 2,2′-dipyridyl (29) after the samples were dissolved in a HCl solution. The crystallite size and morphology of the products were examined by transmission electron microscopy (TEM). The BET surface area was determined by nitrogen adsorption (Shimadzu, Micromeritics Flow Sorb II 2300). The thermal analysis was carried out by using TG-MS (Mac Science, Model TG DTA 2000, and VG Anatech, Model QUADRUPOLES 560) at a heating rate of 20°C min^{-1} in an N_2 gas stream. The lattice constants of the products were calculated by extrapolating the values of a_0 vs the Nelson–Riley function, $\cos^2\theta/\sin\theta + \cos^2\theta/\theta$, to zero using the least-squares method (30). The average crystallite size, D, was determined using Scherrer's equation from the line broadening of the XRD peak for the (311) plane of the spinel structure (31).

3. Catalytic Experiments

Catalytic reactions were carried out in a continuous-flow fixed bed. A 1.0-g portion of the Ni(II) ferrite catalyst was packed in a quartz tube with a diameter of 8 mm and a length of 330 mm. The reaction tube was heated in an electric furnace to allow reaction with gases. The temperature was controlled within ± 0.3°C using a regulator (Chino, Model DB1150) equipped with a chromel–alumel thermocouple. Methanation of CO_2 was studied while a mixed gas of H_2 and CO_2 was passed at a constant flow rate of 25 cm^3 min^{-1} through the ferrite at 300°C. The mole ratio of H_2 to CO_2 was adjusted to 4. The gaseous effluent from the reaction tube was determined by gas chromatography (Shimadzu, Model GC-8A) equipped with Porapak Q or Molecular Sieve 13X column and TCD detector. The amount of carbon deposited on the surface of the solid phase was determined by an elemental analyzer (Perkin-Elmer, Model 2400 CHN).

The solid phase of the ferrite catalyst used for methanation was identified by XRD with Cu$K\alpha$ radiation. The catalyst was quenched by quickly placing the reaction tube in the refrigerant of ice. It was taken out of the reaction tube in a nitrogen atmosphere, mounted on the glass plate, and then covered by a polyethylene film in order to prevent oxidation of the sample. The chemical composition of the ferrite was determined by colorimetry using 2,2′-dipyridyl for the mole ratio of Fe^{2+} and by ICP-AES for content of the total Fe.

RESULTS AND DISCUSSION

1. Synthesis and Characterization of Ni(II) Ferrite Catalysts

NF gave only peaks of the spinel-type structure (Fig. 1a). No other peaks assigned to α-Fe_2O_3 or other compounds

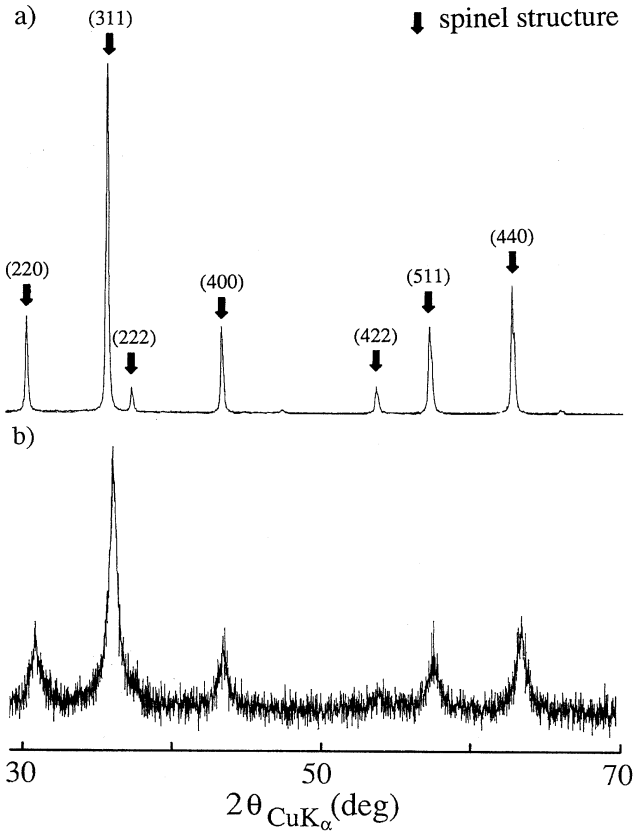

FIG. 1. XRD patterns of Ni(II) ferrites prepared by oxidation (a) and by coprecipitation (b).

were observed. The XRD pattern of UNF also corroborated that the UNF was a single phase with the spinel structure (Fig. 1b). The line broadening observed in the pattern (b) is due to the small crystallite size. The average crystallite size was calculated to be 16 nm for the UNF from the (311) plane.

Figure 2a shows a TEM photograph of NF obtained by the heat treatment of the precipitate formed after the oxidation of Fe(II) and Ni(II) hydroxide suspensions. The particles were nearly spherical and the crystallite size ranged from 100 to 200 nm. It was difficult to prepare ultrafine particles with crystallite size less than 50 nm by this oxidation method. The coprecipitation of Ni^{2+}, Fe^{2+}, and Fe^{3+} was able to give ultrafine particles with size less than 50 nm. After heat treatment, the coprecipitate was made up of nearly spherical and ultrafine particles of size on the order of 10 to 20 nm (Fig. 2b). This result was basically consistent with the XRD studies.

TABLE 1

Chemical Compositions, Lattice Constants (a_0), and Average Crystallite Sizes (D) of Ni(II) Ferrites Prepared by Oxidation (NF) and Coprecipitation (UNF)

Sample	Chemical composition	a_0 (nm)	D (nm)	S_{BET} ($m^2\ g^{-1}$)
NF	$Ni^{2+}_{0.39}\ Fe^{2+}_{0.59}\ Fe^{3+}_{2.02}O_{4.01}$	0.8376	200	9
UNF	$Ni^{2+}_{0.36}\ Fe^{2+}_{0.45}\ Fe^{3+}_{2.19}O_{4.10}$	0.8372	16	73

Since the average crystallite size of UNF was about 1/9 of that of NF (UNF, 16 nm; NF, 150 nm), the surface area of UNF should be 9 times as large as that of NF. The BET surface areas (S_{BET}) of NF and UNF were estimated to be 9 and 73 $m^2\ g^{-1}$, respectively (Table 1). The S_{BET} of UNF was 8 times as large as that of NF, which is consistent with their crystallite sizes.

The NF and UNF showed an ^{57}Fe absorption Mössbauer spectrum consisting of two sextets at room temperature (Fig. 3). The profiles were characteristic of ferrite compounds with crystal structure of the spinel type (32). These two sextets were due to iron ions in tetrahedral (A) and octahedral (B) sites. The Mössbauer spectrum of the UNF was broad at room temperature (Fig. 3b). The broadened peaks of the absorption are characteristic of ferromagnetic ferrites with the small crystallite size. This broadening prevented computer curve fitting of the spectrum.

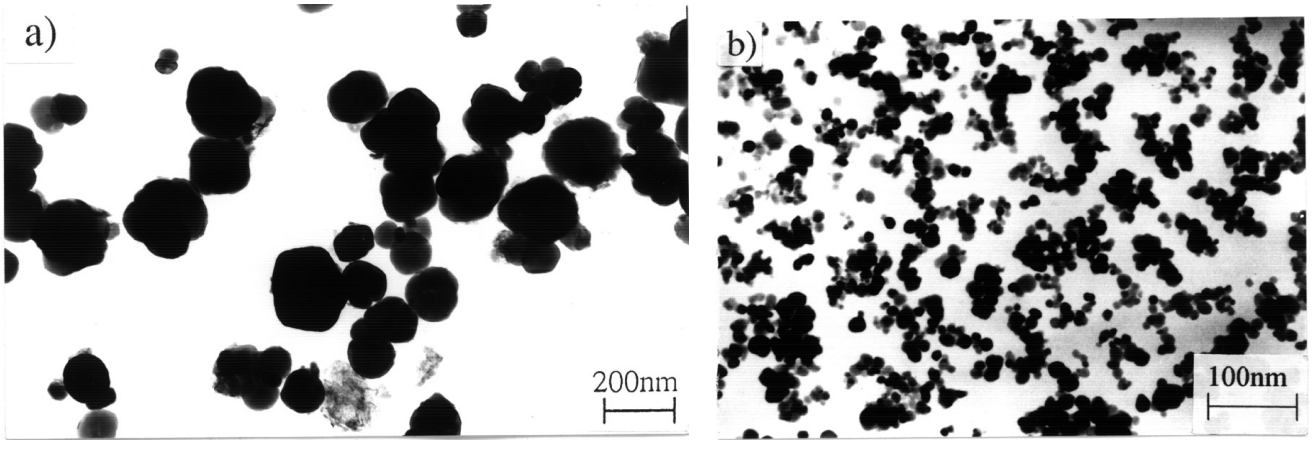

FIG. 2. TEM photographs of Ni(II) ferrites prepared by oxidation (a) and by coprecipitation (b).

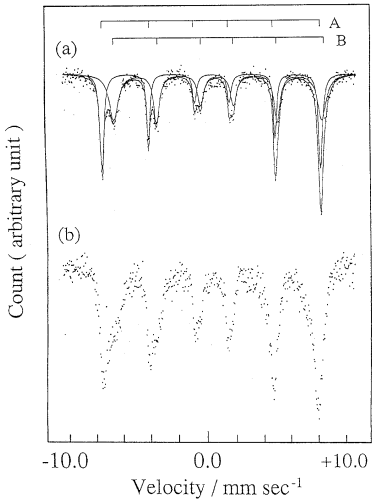

FIG. 3. Mössbauer spectra of Ni(II) ferrites prepared by oxidation (a) and by coprecipitation (b).

The chemical composition of the NF was nearly the stoichiometric composition of $Ni_xFe_{3-x}O_4$ (Table 1, NF). The Ni/Fe mole ratio of the NF (0.149) was nearly the same as that of the starting solution for the preparation (0.15), indicating that the whole mass of the coprecipitate was crystallized to form the spinel-type compound. The chemical composition of the UNF was rather oxidized (Table 1, UNF). The Ni/Fe mole ratio of the UNF (0.136) was smaller than that of the starting solution for the coprecipitation. Not all Ni^{2+} ions in the starting solution were incorporated into the crystal structure of the spinel type. The a_0 of the NF was 0.8376 nm, which was nearly equal to that of the Ni(II) ferrite with 39% Ni^{2+} substitution (0.8376 ± 0.0001 nm) (16–18). The a_0 of the UNF (0.8372 nm) was much smaller than that of the Ni(II) ferrite with 36% Ni^{2+} substitution (0.8377 ± 0.0001 nm). The UNF was oxidized in comparison with the stoichiometry. This resulted in the smaller lattice constant.

In the IR spectra of the NF and UNF, absorption bands characteristic of ferrites were observed at 570 and 360 cm^{-1} (Fig. 4). The former band is assigned to the vibration of the oxygen ion along the tetrahedral bond, and the latter is due to the motion of the oxygen ion in a direction almost perpendicular to the tetrahedral bond (33). The IR spectra did not show any absorption bands at 800–1100 cm^{-1}, indicating the absence of by-products of iron oxide hydroxides such as α-FeO(OH) or $Ni(OH)_2$ (34). The absorption bands at 1630 and 3440 cm^{-1} in spectrum (b) can be assigned to the stretching vibrations and the deformation of H_2O (Fig. 4b). These absorption bands also stem from the OH groups. This result indicates that H_2O and OH groups are included in the UNF of the coprecipitate of Ni^{2+}, Fe^{2+}, and Fe^{3+}.

Figure 5 shows the TG curve of the coprecipitate of Ni^{2+}, Fe^{2+}, and Fe^{3+} before heat treatment. The weight of the coprecipitate decreased in the N_2 gas stream in the temperature range from 40 to 400°C. The weight loss was 6.0 wt%. The effluent gases of H_2O and CO_2 were detected by mass spectrometry, which indicates that the release of these gases from the coprecipitate give rise to the weight loss of the coprecipitate. Most of the weight loss of 6.0 wt% corresponded to the amount of H_2O evolved (5.5 wt%) and the rest to that of CO_2 evolved (0.5 wt%). The water evolution will be due to desorption of adsorbed water and/or dehydration of OH group in the coprecipitate. Such a water is considered as released by the heat treatment in the process of the preparation. However, a part of this may remain in the coprecipitate. So the adsorption bands assigned to the H_2O or OH groups are considered as observed in the IR spectrum of the UNF. More detailed discussion on the characterization of the coprecipitate and on the formation of the ultrafine Ni(II) ferrite will be published elsewhere.

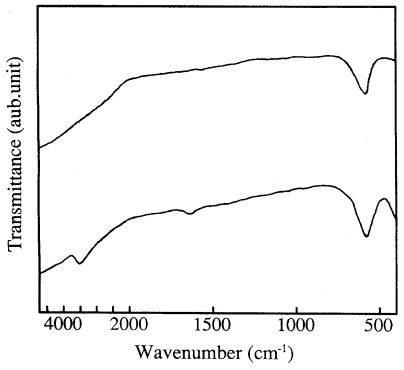

FIG. 4. IR spectra of Ni(II) ferrites prepared by oxidation (a) and by coprecipitation (b).

Thus, it can be concluded that ultrafine Ni(II) ferrite (UNF) with a large surface area of 73 $m^2\ g^{-1}$ has been synthesized by aging a coprecipitate of Ni^{2+}, Fe^{2+}, and Fe^{3+}, followed by heat treatment at 300°C.

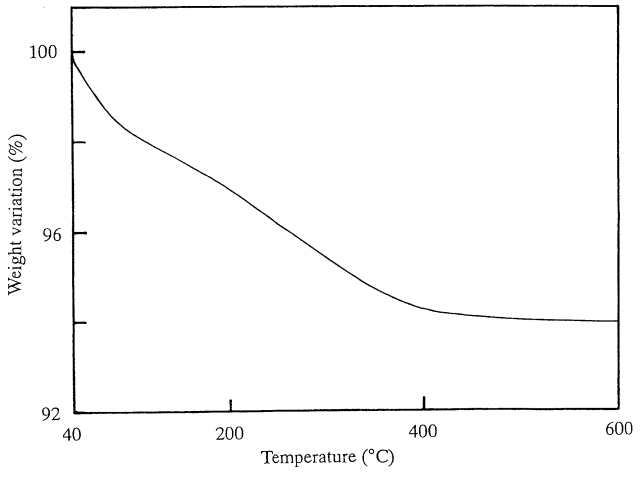

FIG. 5. TG curve of coprecipitate of Ni^{2+}, Fe^{2+}, and Fe^{3+} while heating to 600°C at 2.5°C min^{-1} and passing an N_2 gas at a flow rate of 50 $cm^3\ min^{-1}$.

TABLE 2

Conversion of CO_2, Yield and Selectivity of Gaseous Products in CO_2 Methanation Using NF and UNF Catalysts after a 2-h run[a]

Sample	Conversion of CO_2 (%)	Yield (%)		Selectivity (%)	
		CH_4	CO	CH_4	CO
NF	30.9	25.1	5.3	81.3	17.0
UNF	38.7	37.3	1.1	96.4	2.8

[a] Reaction conditions: catalyst weight = 1.0 g, temperature = 300°C, mole ratio of reactant H_2/CO_2 gas = 4, flow rate of the reactant gas = 25 cm^3 min^{-1}.

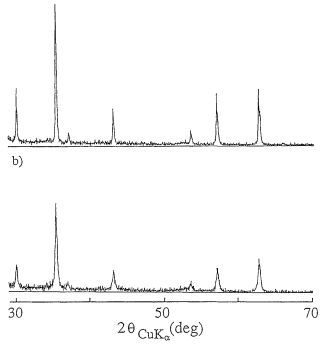

FIG. 6. XRD patterns of the solid phases of NF (a) and UNF (b) catalysts after 2 h of CO_2 methanation at 300°C.

2. Catalytic Results

CH_4, C_2H_6, and/or CO was formed by passing the mixed gas of H_2 and CO_2 through the ferrite catalysts at 300°C. The yield for each chemical species was defined by the mole ratio of the species of interest to the sum of all carbonaceous species in the effluent gases. The selectivity for each product was defined by the mole ratio of the species of interest to all carbonaceous products. The amount of C_2H_6 evolved was about 1/100 of that of the main product, CH_4, and was negligible.

Table 2 shows conversion of CO_2, and yields and selectivities for CH_4 and CO over the ferrite catalysts for a 2-h run of CO_2 methanation. The CO_2 conversion using UNF was higher than that using NF. The yield of CH_4 increased to 37% with UNF in comparison with 25% with NF. The CH_4 yields for 2-h runs on UNF and NF linearly decreased to 12 and 2%, respectively, with an increase in flow rate of reactant H_2/CO_2 mixed gas from 25 to 100 cm^3 min^{-1}. The CH_4 yield on UNF was 1.5–6.0 times larger than that on UNF, depending on the flow rate. On the other hand, the yield of CO obtained on the UNF was about 1.1% and lower than that obtained on the NF (17%), as shown in Table 2. Accordingly, selectivity for CH_4 was improved with the UNF catalyst, increasing from 81 to 96%. The Ni^{2+} substitution in the NF and UNF was nearly the same: $x = 0.39$ and 0.36, respectively. Hence, it can be considered that the ferrite particle size controlled in nanoscale gave rise to the improvement of the methanation selectivity.

After a 2-h methanation run, the UNF showed the XRD pattern assigned to the spinel-type compound (Fig. 6b). No evidence of FeO, NiO, metallic iron, or nickel was observed in the XRD pattern of the UNF. The elemental analysis of the UNF after methanation for 2 h showed that carbon deposition did not take place on UNF. The phase of the UNF catalyst during the methanation is considered to consist of the single phase of the spinel-type structure. Its lattice constant increased from 0.8372 to 0.8380 nm during the methanation (Tables 1 and 3; UNF). This increase in the lattice constant came from the change in the ionic radius associated with the reduction of Fe^{3+} to Fe^{2+} and/or the cation repulsion arising from the presence of excess iron ions in the interstices of the spinel-type structure. The chemical composition of UNF was changed to the composition of the reduced form in comparison with the stoichiometry (Table 3; UNF). These results suggest that the UNF was transformed to oxygen-deficient ultrafine Ni(II) ferrite (ODUNF) during the methanation. The oxygen deficiency, δ value in $Ni_xFe_{3-x}O_{4-\delta}$, of the ODUNF was kept constant in the course of the methanation after 15 min up to 2 h. This indicates that catalytic conversion of CO_2 to CH_4 occurred on the ODUNF catalyst. A similar phenomenon took place in the NF (Fig. 6a and Tables 1 and 3; NF). The NF was also transformed to the oxygen-deficient form. Its δ value was much smaller than that of the UNF (Table 3).

Tamaura *et al*. pointed out that the oxygen-deficient ferrite had a high reduction potential because of its distorted spinel structure in comparison with the stoichiometric compound (1, 2). So it is very reactive with CO_2 and can incorporate O^{2-} ions from the CO_2 into the oxygen sublattice. Kato *et al*. reported the methanation of CO_2 using the oxygen deficient Ni(II) ferrite (ODNF) (16–18). The methanation of CO_2 on the ODNF is considered to involve three elementary reactions: (1) release of a lattice oxygen with hydrogen to form an oxygen-sublattice point on the surface of the ODNF, (2) incorporation of oxygen ions of CO_2 into the oxygen-sublattice points to form an adsorbed atomic carbon on the surface of the ODNF, and (3) hydrogenation of

TABLE 3

XRD Patterns, Lattice Constants (a_0), Chemical Compositions, δ Values and BET Surface Area (S_{BET}) of the Ni(II) Ferrite Catalysts for a 2 h-run of the Methanation[a]

Sample	XRD pattern	a_0 (nm)	Chemical composition	δ	S_{BET} (m^2 g^{-1})[b]
NF	Spinel	0.8378	$Ni^{2+}_{0.39}$ $Fe^{2+}_{0.84}$ $Fe^{3+}_{1.77}O_{3.89}$	0.11	9
UNF	Spinel	0.8380	$Ni^{2+}_{0.36}$ $Fe^{2+}_{1.07}$ $Fe^{3+}_{1.57}O_{3.79}$	0.21	26

[a] Reaction conditions: temperature = 300°C, mole ratio of reactant H_2/CO_2 gas = 4, flow rate of the reactant gas = 25 cm^3 min^{-1}.

[b] BET surface areas of the catalysts for a 1-h run of the methanation.

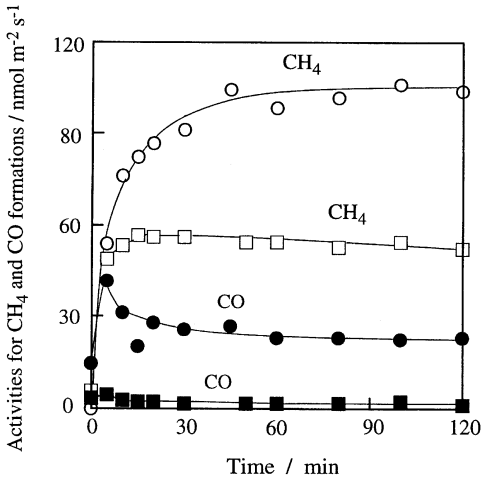

FIG. 7. Time variation of the specific activities of NF (circle) and UNF (square) catalysts for CH_4 (open) and CO (solid) formations at 300°C. Reaction condition: catalyst weight = 1.0 g, mole ratio of H_2 to CO_4 = 4, and a flow rate = 25 cm^3 min^{-1}.

the atomic carbon to form CH_4. These elementary reactions can be formulated as

$$H_2 + O^{2-}_{lat} + 2Fe^{3+}_{lat} \rightarrow H_2O + Vo + 2Fe^{2+}_{int} \quad [1]$$

$$CO_2 + 2Vo + 4Fe^{3+}_{int} \rightarrow C_{ads} + 2O^{2-}_{lat} + 4Fe^{3+}_{lat} \quad [2]$$

$$C_{ads} + 2H_2 \rightarrow CH_4, \quad [3]$$

where O^{2-}_{lat} and Fe^{3+}_{lat} denote an oxygen ion and a trivalent iron ion in the normal positions for the spinel structure, respectively, Vo and Fe^{2+}_{int} represent a sublattice point of oxygen and a bivalent iron ion in the interstices of the spinel structure, respectively, and C_{ads} denotes an adsorbed atomic carbon on the surface of the ODNF. The methanation of CO_2 occurring on the oxygen-deficient ultrafine Ni(II) ferrite (ODUNF) will involve the same elementary reactions. The elementary reaction (2) is considered the rate-determining step on UNF because no carbon deposition was detected on the solid phase during the CO_2 methanation.

After a 1-h methanation run, the S_{BET} of UNF significantly decreased from 73 to 26 m^2 g^{-1}, while that of NF remained unchanged (9 m^2 g^{-1}) (Tables 1 and 3). After the rapid decrease in the S_{BET} of UNF, it did not greatly change up to 10 h (S_{BET} = 20 m^2 g^{-1} for a 10-h run). These results imply that the sintering of the UNF occurred rapidly in the initial stage of the reaction, probably in heating to 300°C, and then did not appreciably proceed at a constant temperature of 300°C.

Specific activities (nmol m^{-2} s^{-1}) of both catalysts for CH_4 and CO formations were estimated using the S_{BET} observed after a 1-h methanation run and plotted as a function of reaction time in Fig. 7. The activity of UNF for CH_4 formation was about one-half the activity of NF. This comes from the fact that the surface density of active sites for methanation on UNF was lower than that on NF, as follows: The oxygen deficiency of UNF was 1.9 times as large as that of NF; however, the S_{BET} of the UNF was 2.9 times larger than that of NF, as shown in Table 3. Therefore, the surface density of oxygen sublattice for UNF should be 65% of that of NF. If oxygen sublattice points formed on the ferrite surface by H_2 reduction serve as active sites for methanation, as shown by the elementary reactions, the specific activity of UNF becomes about half the activity of NF. On the other hand, the activity for CO formation significantly decreased for UNF in comparison with NF. We reported that CO_2 can be readily decomposed to carbon and oxygens when the oxygen deficiency of ferrite is high (1–10). However, with a low oxygen deficiency, the reduction of CO_2 to CO is dominant. Since UNF has a much higher oxygen deficiency than NF, the selectivity for CO_2 decomposition to atomic carbon will be improved on the UNF surface. This enhancement of CO_2 decomposition to carbon would lower the activity for CO formation.

The activity for CH_4 formation shown in Fig. 7 was retained for a 10-h run on NF. However, the activity of UNF for CH_4 gradually decreased and reached 30 nmol m^{-2} s^{-1} after a 10-h run. In the XRD pattern of UNF after a 10-h methanation, small and broad peaks assigned to metallic Ni or Fe appeared along with strong spinel peaks, although the NF after 10 h of methanation showed only the spinel peaks. The ODUNF would be deactivated by the formation of metallic phase on the catalyst surface. Since the ODUNF has a higher δ than that of ODNF, the spinel lattice of ODUNF is more distorted and unstable in comparison with ODNF. Thus, the transformation of oxygen-deficient ferrite to metallic phase will more readily occur in ODUNF. The ODUNF with metallic phase will be reactivated by reoxidation treatment.

Figure 8 shows a relationship between the flow rate of the reactant gas (H_2/CO_2 mixed gas) and the specific activity of

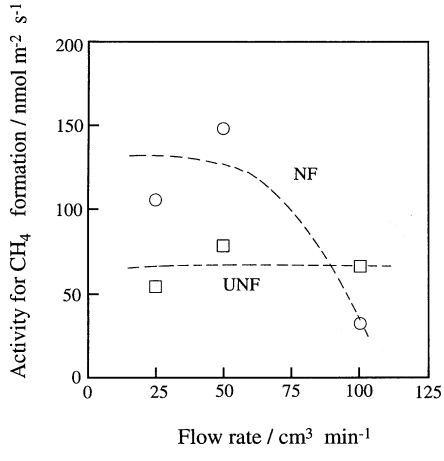

FIG. 8. Relationship between the specific activity for CH_4 formation and the flow rate of reactant H_2/CO_2 mixed gas for a 2-h run of the methanation at 300°C. Circle marks are for NF and square for UNF.

catalysts for CH_4. The NF showed the activity twice as large as the UNF in the flow rate of 25–50 $cm^3\ min^{-1}$. The activity of UNF was retained at a high flow rate of 100 $cm^3\ min^{-1}$. However, that of NF significantly decreased and the UNF rather showed a higher activity than the NF at the high flow rate. The ODNF with a lower δ than ODUNF may be readily oxidized at a high flow rate of CO_2 to decrease the active sites of oxygen sublattice points.

CONCLUSIONS

Ultrafine Ni(II) ferrite (UNF) could be synthesized by aging a coprecipitate of Ni^{2+}, Fe^{2+}, and Fe^{3+}, followed by heat treatment at 300°C. The crystallite size of 10–20 nm was an order of magnitude larger than that of the Ni(II) ferrite (NF) synthesized by the conventional oxidation method. The BET surface area of the UNF was initially 73 $m^2\ g^{-1}$. However, it rapidly decreased to 26 $m^2\ g^{-1}$ by sintering during CO_2 methanation at 300°C, being twice as large as that of the NF. The yield of CH_4 obtained on the UNF catalyst was about 1.5–6.0 times as large as that obtained on the NF, depending on the flow rate of reactant H_2/CO_2 mixed gas. It was found that UNF showed a higher catalytic selectivity than the NF for CO_2 methanation. During the methanation, both the NF and the UNF were transformed to the reduced form (oxygen-deficient ferrite) in which the metallic phase was not involved and the spinel structure was distorted by the release of the lattice oxygen. The specific activity ($mol\ m^{-2}\ s^{-1}$) of UNF for CH_4 formation was about half that of NF, which could be explained assuming that oxygen sublattice points on the catalyst surface formed by H_2 reduction serve as active sites for methanation. On the other hand, the activity for CO formation significantly decreased on UNF, which would be due to the change in the nature of active site.

REFERENCES

1. Tamaura, Y., and Tabata, M., *Nature* **346**, 255 (1990).
2. Nishizawa, K., Kodama, T., Tabata, M., Yoshida, T., Tsuji, M., and Tamaura, Y., *J. Chem. Soc. Faraday Trans.* **88**, 2771 (1992).
3. Tamaura, Y., and Nishizawa, K., *Energy Convers. Mgmt.* **33**, 573 (1992).
4. Tabata, M., Nishida, Y., Kodama, T., Mimori, K., Yoshida, T., and Tamaura, Y., *J. Mater. Sci.* **28**, 971 (1993).
5. Tabata, M., Akanuma, K., Nishizawa, K., Mimori, K., Yoshida, T., Tsuji, M., and Tamaura, Y., *J. Mater. Sci.* **28**, 6753 (1993).
6. Akanuma, K., Nishizawa, K., Kodama, T., Tabata, M., Mimori, K., Yoshida, T., Tsuji, M., and Tamaura, Y., *J. Mater. Sci.* **28**, 860 (1993).
7. Akanuma, K., Tabata, M., Hasegawa, N., Tsuji, M., Tamaura, Y., Nakahara, Y., and Hoshino, S., *J. Mater. Chem.* **3**, 943 (1993).
8. Kato, H., Kodama, T., Tsuji, M., Tamaura, Y., and Chang, S. G., *J. Mater. Sci.* **29**, 5689 (1994).
9. Kodama, T., Kato, H., Chang, S. G., Hasegawa, N., Tsuji, M., and Tamaura, T., *J. Mater. Res.* **9**, 462 (1994).
10. Tabata, M., Akanuma, K., Togawa, T., Tsuji, M., and Tamaura, Y., *J. Chem. Soc. Fraday Trans.* **90**, 1171 (1994).
11. Yoshida, T., Nishizawa, K., Tabata, M., Abe, H., Kodama, T., Tsuji, M., and Tamaura, Y., *J. Mater. Sci.* **28**, 1220 (1993).
12. Nishizawa, K., Kato, H., Mimori, K., Yoshida, T., Hasegawa, N., Tsuji, M., and Tamaura, Y., *J. Mater. Sci.* **29**, 768 (1994).
13. Tsuji, M., Nishizawa, K., Yoshida, T., and Tamaura, Y., *J. Mater. Sci.* **29**, 5481 (1994).
14. Tsuji, M., Kato, H., Kodama, T., Chang, S. G., Hasegawa, N., and Tamaura, Y., *J. Mater. Sci.* **29**, 6227 (1994).
15. Kodama, T., Kato, H., Tsuji, M., Tamaura, Y., and Chang, S. G., *in* "Proceedings of World Congress III on Engineering and Environment" (Q. Yi, H. Jiming, and L. Jun, Eds.), Vol. 2, p. 518. International Academic Publishers, Beijing, 1993.
16. Kato, H., Tamaura, Y., Tsuji, M., Tsuji, T., and Miyazaki, S., *in* "Proc. Int. Symp. on CO_2 Fixation & Efficient Utilization" (Y. Tamaura, K. Okazaki, M. Tsuji, and S. Hirai, Eds.), p. 215. Research Center for Carbon Recycling & Utilization, Tokyo, 1993.
17. Kato, H., Tabata, M., Tsuji, M., and Tamaura, Y., *in* "Mat. Res. Soc. Symp. Proc." (K. E. Voss, L. M. Quick, P. N. Gadgil, and C. L. J. Adkins, Eds.), Vol. 344, p. 163. Materials Research Society, Pittsburgh, 1994.
18. Kato, H., Sano, T., Wada, Y., Tamaura, Y., Tsuji, M., Tsuji, T., and Miyazaki, S., *J. Mater. Sci.* **30**, 6350 (1995).
19. Kiyama, M., *Bull. Chem. Soc. Jpn.* **47**, 1646 (1974).
20. Kiyama, M., *Bull. Chem. Soc. Jpn.* **51**, 134 (1978).
21. Kanzaki, T., Nakajima, J., Tamaura, Y., and Katsura, T., *Bull. Chem. Soc. Jpn.* **54**, 135 (1981).
22. Kaneko, K., and Katsura, T., *Bull. Chem. Soc. Jpn.* **52**, 747 (1979).
23. Kaneko, K., Takei, K., Tamaura, Y., Kanzaki, T., and Katsura, T., *Bull. Chem. Soc. Jpn.* **52**, 1080 (1979).
24. Tamaura, Y., and Katsura, T., *J. Chem. Soc. Dalton Trans.* 825 (1980).
25. Kanzaki, T., Furukawa, H., and Katsura, T., *J. Chem. Soc. Dalton Trans.* 1197 (1983).
26. Tamaura, Y., Rasyid, U., and Katsura, T., *J. Chem. Soc. Dalton Trans.*, 2125 (1980).
27. Tamaura, Y., Mechaimonchit, S., and Katsura, T., *J. Inorg. Nucl. Chem.* **43**, 671 (1981).
28. Katsura, T., Tamaura, Y., and Chyo, G. S., *Bull. Chem. Soc. Jpn.* **52**, 96 (1979).
29. Snell, F. D., and Snell, C. T., "Colorimetric Methods of Analysis," Vol. 1 Inorganic, p. 310. Van Nostrand, New York, 1953.
30. Nelson, J. B., and Riley, D. P., *Proc. Phys. Soc. London* **57**, 160 (1945).
31. West, A. R., Solid State Chemistry and Its Applications, Wiley, p. 173. New York, 1984.
32. Robbins, M., Wertheim, G. K., Sherwood, R. C., and Buchanan, D. N. E., *J. Phys. Chem. Solids* **32**, 717 (1971).
33. Waldron, R. D., *Phys. Rev.* **99**, 1727 (1955).
34. Misawa, T., Hashimoto, K., and Shimodaira, S., *Boshoku Gijutsu (Corrosion Engineering)* **23**, 17 (1974).